

POLITECNICO
MILANO 1863

Master of Science in Space Engineering

**Spacecraft Attitude Dynamics
Academic Year 2023/24**

Project Group n. 38

Project n. 150

Professor: Bernelli Zazzera Franco

Team members:

Person Code	Surname	Name	Bachelor
10627453	Baniamein	Mina	Aerospace Engineering - PoliMi
10673485	Bellezza	Alessandro	Aerospace Engineering - PoliMi
10767871	Di Carlo	Pierpaolo	Aerospace Engineering - PoliTo
10582310	Trovatelli	Gaia	Aerospace Engineering - PoliMi

Project specification:

	Assigned Specification	Modifications	Motivation for modification
Platform	6U	-	
Attitude Parameters	DCM Matrix	-	
Mandatory Sensor	Sun Sensor	Added an Earth Horizon Sensor and 3 Gyroscopes (aligned with the 3 body axes)	The EHS is necessary in order to obtain a second measured direction for the Attitude Determination algorithm to completely determine the spacecraft's attitude; the gyroscopes allow the measurement of the angular velocity, which is necessary for the detumbling phase
Actuators	Variable Thrust	-	

Table of contents

1	Spacecraft and Orbit Characterization	1
1.1	Spacecraft reference	1
1.2	Mission and Orbital parameters	2
1.3	Spacecraft Dynamics	3
1.4	Spacecraft Kinematics	3
2	Environment	5
2.1	Disturbances Estimation	5
2.2	Gravity Gradient Torque	6
2.3	Magnetic Torque	6
3	Sensors and Actuators	8
3.1	Sun sensors	8
3.2	Horizon sensor	9
3.3	Gyroscopes	10
3.4	Actuators	10
4	Attitude determination	12
4.1	Introduction	12
4.2	Control Algorithms	13
4.2.1	De-tumbling	13
4.2.2	Slew manoeuvre	14
4.3	Nominal control logic	15
4.3.1	References for tracking	15
4.3.2	Control implementation	16
5	Conclusion	17

Chapter 1

Spacecraft and Orbit Characterization

1.1 Spacecraft reference

In order to correctly model the geometrical properties of the assigned satellite type, we referenced the 6U cubesat BioSentinel: the dimensions are the typical 6U satellite $10\text{ cm} \times 20\text{ cm} \times 30\text{ cm}$, with a mass of 14 kg.

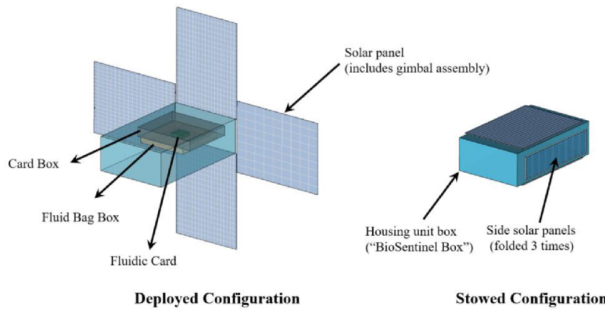


Figure 1.1: BioSentinel configuration

From the geometrical data that we retrieved we can then determine the satellite's Principal Inertia Matrix, by approximating it to a cuboid body rotating around its center of mass, which is coincident with its center of geometry:

$$I_d = \frac{m}{12}(w^2 + h^2) \quad I_w = \frac{m}{12}(d^2 + h^2) \quad I_h = \frac{m}{12}(w^2 + d^2) \quad (1.1)$$

And thus the estimated inertia matrix was determined by arbitrarily setting the z Body Axis to be the maximum inertia axis and the x Body Axis to be the minimum inertia axis:

$$\underline{\underline{J}} = \begin{bmatrix} 0.050566 & 0 & 0 \\ 0 & 0.12641 & 0 \\ 0 & 0 & 0.5517 \end{bmatrix} \quad (1.2)$$

Since the inertia moments are such that $I_z > I_y > I_x$ we have a condition of stability identified by the region (1), as it possible to see in Figure 1.2. The unmarked regions represent the stable regions, while the remaining regions present some kind of instability.

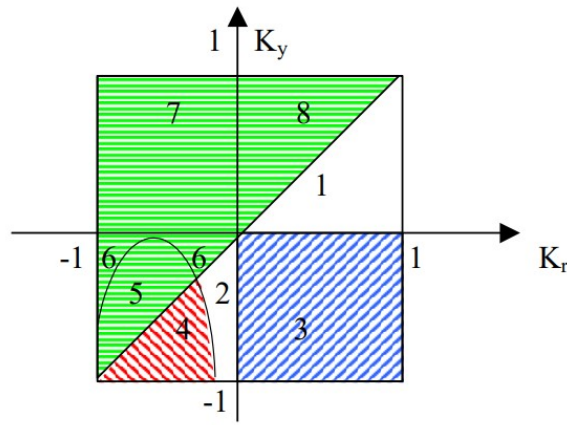


Figure 1.2

1.2 Mission and Orbital parameters

The orbital parameters chosen are greatly influenced by the decision to perform an Earth Observation Mission, leading to the choice of a circular polar orbit: this allows for the continuous use of the Sun Sensor during the entirety of the nominal mission, with an additional advantage in the possibility for data transfer when above the North Pole. Therefore, the following orbital parameters have been chosen:

Semi Major Axis (a)	7136.6 km
Eccentricity (e)	0
Inclination (i)	90°
Right Ascension of the Ascending Node (Ω)	90°
Anomaly of pericenter (ω)	0

Table 1.1: Orbital parameters

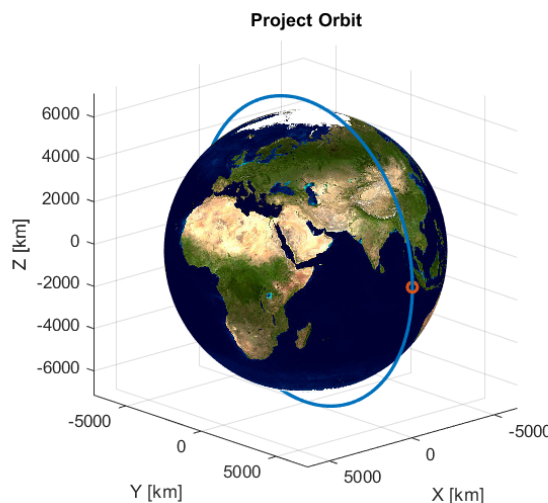


Figure 1.3: Chosen orbit with Starting Point

The choice of a zero-eccentricity orbit makes it more stable under the perturbations that were neglected in the following analysis, making the model more reliable and less subject to errors, while the inclination and RAAN (Ω) choices guarantee an absence of eclipse time in the orbit, under the assumption that the Sun is located along the \hat{X} direction of the Earth-Centered Inertial Frame, with the additional possibility to obtain a Sun-synchronous orbit that will preserve this condition indefinitely with minimal changes (typical Sun-synchronous orbits are characterized by the same altitude and an inclination of about 98°), allowing for the same overall architecture to work as well.

Furthermore, the choice of which body axis will be pointed in the Nadir direction allowed us to exploit another characteristic of LEOs: since the Gravity gradient perturbation is usually predominant in such situations, we decided to use this perturbation as a stabilizing factor by pointing the minimum inertia axis in the radial direction during the nominal phase of the mission, allowing us to reduce the necessary control power once the attitude is sufficiently close to the target.

1.3 Spacecraft Dynamics

The dynamics of the spacecraft has been simulated with the assumption of having a 6 DoF rigid body. The translational dynamics is simulated using an unperturbed restricted two body problem with initial conditions corresponding the position and velocity at the pericenter of the orbit:

$$\ddot{\underline{r}} = -\frac{\mu}{r^3} \underline{r} \quad (1.3)$$

The rotational dynamics is described by Euler's equations:

$$\underline{J}\dot{\underline{\omega}} + \underline{\omega} \times \underline{J}\underline{\omega} = \underline{T} \quad (1.4)$$

Where in our implementation both these equations have been integrated numerically, using the differential equation solving algorithm based on Runge-Kutta's method (ode4).

1.4 Spacecraft Kinematics

In order to simulate the Kinematics, the Director Cosines Matrix (DCM) has been used, specifically the rotation matrix between the always known Earth-centered inertial Frame (from here on will be indicated with the notation 'N', or X_N, Y_N, Z_N) and the body frame (indicated as 'B', or x_B, y_B, z_B).

By definition, this rotation matrix will be determined as the 3×3 matrix whose rows are composed by the three versors composing the base of the body frame ($\underline{e}_{1,B}, \underline{e}_{2,B}, \underline{e}_{3,B}$) expressed in components in the inertial frame:

$$\underline{\underline{A}}_{B/N} = \begin{bmatrix} \underline{e}_{1,B} \\ \underline{e}_{2,B} \\ \underline{e}_{3,B} \end{bmatrix} \quad (1.5)$$

Consequentially, it's now necessary to relate the change of the attitude parameters with respect to the angular velocity of the body, which is now known through the Dynamics Equations Solution:

$$\frac{dA}{dt} = f(w_x, w_y, w_z) \quad (1.6)$$

where the angular velocity's components are measured in Body Frame.

If matrix A is known at a certain time instant, then it's possible to evaluate the DCM after a discrete interval through the rule of consecutive rotations, by defining the matrix A' as the rotation occurred in the time interval Δt :

$$A(t + \Delta t) = A' \cdot A(t) \quad (1.7)$$

By expressing the matrix A' as a function of Euler axis and angle in the interval Δt :

$$A' = I \cos \Phi + (1 - \cos \Phi) \underline{e} \underline{e}^T - \sin \phi [\underline{e} \wedge] \quad (1.8)$$

Then by using the definition of derivative, and thus setting the time interval to approach zero, the previous expression will be further simplified as ϕ can be considered small:

$$A' = I - \Phi [\underline{e} \wedge] \quad (1.9)$$

For such small rotations Euler axis will be coincident with the angular velocity vector direction:

$$\Phi = \omega \delta t \quad (1.10)$$

$$\underline{\omega} = \omega \underline{e} \quad (1.11)$$

$$\Phi [\underline{e} \wedge] = \omega \Delta t \begin{bmatrix} 0 & -e_z & e_y \\ e_z & 0 & -e_x \\ -e_y & e_x & 0 \end{bmatrix} = \begin{bmatrix} 0 & -\omega_z & \omega_y \\ \omega_z & 0 & -\omega_x \\ -\omega_y & \omega_x & 0 \end{bmatrix} \Delta t = [\underline{\omega} \wedge] \Delta t \quad (1.12)$$

Applying the definition of derivative, we have then:

$$\frac{dA}{dt} = -[\underline{\omega} \wedge] A(t) \quad (1.13)$$

Since ω is known, the previous equation can be integrated numerically to determine $A(t)$ at every time-step of the integration.

Since the numerical algorithm will introduce errors, to ensure that the solution is physically relevant, the orthogonality of the DCM must be preserved through an iterative method that will not be derived explicitly here but has been implemented in our model.

Chapter 2

Environment

The Environment Model is used in our representation to simulate the external influences on the control logic and related subsystems: this chapter will review the non-neglectable disturbances which were modeled in our approximation of the real forces and torques acting on the real case.

2.1 Disturbances Estimation

The chosen orbit for the mission is a Polar Circular LEO, and together with the small overall size of the spacecraft considered in the analysis, a quick preliminary estimation can verify the impact of the main disturbance phenomena on the attitude control problem.

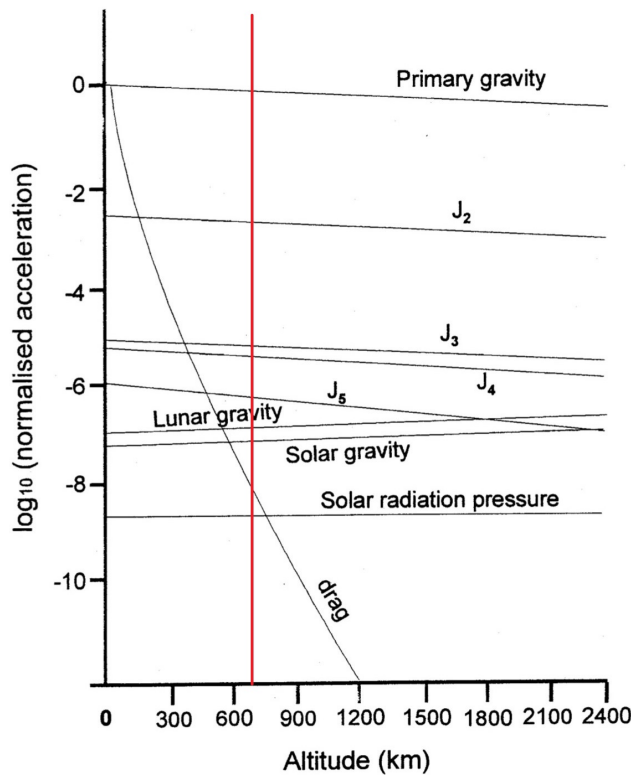


Figure 2.1: Orders of magnitude of the disturbances as the altitude varies

Perturbation	Estimation Formula	Results
Magnetic Torque	$T_{max} = m_{sat}B_{max}$	2.8579e-06 Nm

Table 2.1: Magnetic Torque Disturbance Estimation

From this graph, we can clearly see that the Aerodynamic Drag and Solar radiation Pressure are comparable or lower than the Moon and Sun influence, and can thus be neglected as the latter two. We can then evaluate the Magnetic Torque Perturbation contribution by using an estimation formula:

$$T_{max} = m_{sat}B_{max} \quad (2.1)$$

Where the geometrical parameters were obtained with reference to the BioSentinel 6U CubeSat and the typical LEO satellite values ($B_{max} = 5.5 \cdot 10^{-5} T$), and m_{sat} is the norm of the spacecraft's residual dipole, determined through the NASA SP-8018 Report Tables. From the presented results, as the orbit is low enough and the surface to mass ratio of the spacecraft is relatively high, the predominant disturbances have been found to be The Gravity Gradient and Magnetic Torques.

2.2 Gravity Gradient Torque

The non-uniformity of the gravity field causes a continuous disturbance which effects perpetuated over time may be of primary importance, in particular for larger spacecrafts. When modeling this disturbance, the Earth was considered as a perfect sphere and its oblateness and surface irregularities were neglected. The gravity gradient torque was therefore evaluated in the principal inertia axes as:

$$\underline{T}_{GG} = 3 \frac{Gm_{earth}}{\|\underline{r}\|^3} (\hat{\underline{r}}_B \times \underline{J} \hat{\underline{r}}_B) \quad (2.2)$$

Where $G = 66743 \cdot 10^{-11} \frac{m^3}{kg \cdot s^2}$ is the Universal Gravitational Constant, m_{earth} is the mass of the Earth, \underline{J} is the Principal Inertia Matrix previously determined in chapter 1, $\|\underline{r}\|$ is the radius of the orbit and $\hat{\underline{r}}_B$ is the direction of the position vector of the S/C in Body Frame.

2.3 Magnetic Torque

The torque generated by the Magnetic Disturbance Torque is given by the following equation:

$$\underline{T}_m = \underline{m} \times \underline{B}_B \quad (2.3)$$

Where \underline{m} , the spacecraft dipole moment, is an undesired effect which is caused by residual parasitic currents and it cannot be accurately modeled in a simple manner. Therefore we can approximate this effect with the empirical model described in NASA SP-8018 Report (2) to better estimate it.

Table I.—Criteria for Magnetic Properties Control

	Class I	Class II	Class III
Design	Formal specification on magnetic properties control; approved materials and parts lists; cancellation of moments by preferred mounting arrangements and control of current loops.	Advisory specifications and guidelines for material and parts selection. Avoidance of "soft" magnetic materials or current loops and awareness of good design practices.	Nominal control over current loops; guidelines for avoidance of "soft" magnetic materials.
Quality control	Complete magnetic inspection of parts and testing of sub-assemblies.	Inspection or test of suspect parts.	Test of subassemblies that are potentially major sources of dipole moment.
Test and compensation	Deperming either at subassembly or spacecraft level; test of final spacecraft assembly and compensation if required.	Deperming and compensation frequently used.	Test and compensation optional.

Note.—Class I—Magnetic torques dominant when compared with other torques.

II—Magnetic torques comparable to other torques.

III—Magnetic torques insignificant when compared with other torques.

Figure 2.2: NASA SP-8018 Report Table

In our specific case, since the mass of the S/C is relatively low and any disturbance can significantly affect the dynamics, we assumed that the stricter requirements for Magnetic properties Control could be applied, and therefore the parameters for a Class 1 will be applied. The magnetic field of the Earth \underline{B}_B , as a first approximation, can be modeled as a spinning Dipole that will not account for the real magnetic field's non-uniformity.

$$H_0 = ((g^0_1)^2 + (g^1_1)^2 + (h^1_1)^2)^{1/2} \quad (2.4)$$

$$\underline{B}(r) = \frac{R^3 H_0}{r^3} [3(\hat{m} \cdot \hat{r})\hat{r} - \hat{m}] \quad (2.5)$$

Where \hat{r} is the satellite's position verson and \hat{m} is defined as:

$$\hat{m} = \begin{Bmatrix} \sin\theta'_m \cos\alpha_m \\ \sin\theta'_m \sin\alpha_m \\ \cos\theta'_m \end{Bmatrix} \quad (2.6)$$

with:

$$\alpha_m = \alpha_{G0} + \frac{d\alpha_G}{dt}(t - t_0) + \phi'_m \quad (2.7)$$

Where α_{G0} is the right ascension of the Greenwich meridian at the reference time t_0 , $d\alpha_g/dt$ the average rotation speed of the Earth, θ'_m and ϕ'_m give the orientation of the magnetic dipole. Then we have:

$$\theta'_m = \arccos\left(\frac{g^0_1}{H_0}\right) \quad \phi'_m = \arctan\left(\frac{h^1_1}{g^1_1}\right) \quad (2.8)$$

$$\hat{m} \cdot \hat{r} = \hat{r}_x \sin\theta'_m \cos\alpha_m + \hat{r}_y \sin\theta'_m \sin\alpha_m + \hat{r}_z \cos\theta'_m \quad (2.9)$$

We deemed this approximation sufficiently accurate for our purposes, as the intensity of the Magnetic Perturbation for our study case is decisively inferior relative to the Gravity Gradient Perturbation, and thus a greater error would be admissible without compromising the validity of the subsequent considerations.

Chapter 3

Sensors and Actuators

3.1 Sun sensors

The Sun sensors can be used to determine the direction of the Sun, after the conclusion of the de-tumbling manoeuvre. We selected for our mission the S3 (Smart Sun Sensor), provided by Leonardo company. This sensor is a two axes solar sensor based on an Active Pixel Sensor (APS) detector; it has a large dynamic range, providing medium/high accuracy, and a wide FOV (Field Of View), thus combining the functions traditionally performed by separate fine and coarse Sun sensors. The possibility to switch from a "Sun acquisition mode" to a "Sun Tracking mode" allows us to use the same sensor for both the nominal phase and the slew manoeuvre phase.

Since the spacecraft orbits in a circular polar orbit, the Sun remains always visible and therefore it is guaranteed the functioning of the sensor for the entire duration of the nominal phase.

Performance	
FOV	128° x 128°
Accuracy	<0.02°
Resolution	<0.005°

Table 3.1: Smart Sun Sensor performance

As already said, the Sun sensors provides a measure of the relative position of the Sun in the sensor reference, which we have assumed to be the inertial reference. This measurement has to be transformed into information in the satellite reference through a rotation.

The Sun direction in the inertial frame **N** is computed as:

$$S_N = r_{\text{sun}} \begin{bmatrix} \cos(n_{\text{sun}}t) \\ \sin(n_{\text{sun}}t)\cos(\epsilon) \\ \sin(n_{\text{sun}}t)\sin(\epsilon) \end{bmatrix} \quad (3.1)$$

Therefore the Sun direction in the body frame **B** can be obtained multiplying S_N by the rotation matrix $A_{B/N}$:

$$S_B = A_{B/N} S_N \quad (3.2)$$

This information, however, represent an ideal measure.

In order to model a real sensor we introduced some measurement errors:

- Misalignment error: $A_\epsilon = I - [\theta_\epsilon]^\wedge$, where we have assumed $\theta_\epsilon = 0.02^\circ$ due to the sensor accuracy.

- Zero-Order Hold, which mimics the sampling acquisition frequency of the sensor: *Sample time* = 0.1
- Band-Limited White Noise, which represents errors in the values read by the sensors' electronics: *Noise power* = 0.00001 and *Sample time* = 0.1

It is important to notice that, even if the Sun sensors can provide information about the direction of the Sun relative to the spacecraft, it only gives a single vector in space. This information alone doesn't provide the spacecraft's full orientation, as there are three rotational degrees of freedom (roll, pitch, and yaw) that need to be determined. For this reason it has been added to the spacecraft an Earth Horizon Sensor (EHS), which provides the measurement of a second direction in space and therefore ensure the determination of the spacecraft attitude.

3.2 Horizon sensor

The Horizon sensor is used, after the conclusion of the de-tumbling phase, to determine the position of the Earth with respect to the spacecraft. This information, together with the Sun direction provided by the Sun sensors, allows us to completely determine the spacecraft attitude. We decided to use an Horizon Sensor for Nano and Micro Satellites (HSNS) of Solar MEMS, which is a Quad Thermopile sensor for Earth detection and Nadir vector determination, measuring the infrared radiation from Space and from Earth with 4 IR-eyes.

Performance	
FOV of each IR-eye	$\pm 2.5^\circ$
Aperture	$\pm 64^\circ$
Accuracy	<1°

Table 3.2: HSNS performance

Since the mission of the spacecraft is to perform an Earth observation, it has been decided to impose a nadir-pointing. In this condition, one HSNS is enough since one of the spacecraft's faces is always pointing towards the Earth.

The proceedings to model the real sensor measurement is similar to the one of the Sun sensor.

From the two-body problem we can obtain the information about the Earth direction in the inertial frame (r_N), as it has opposite direction but same modulus of the position vector of the spacecraft. Once we have r_N , it is possible to obtain r_B :

$$r_B = A_{B/N} r_N \quad (3.3)$$

This ideal value can be used to model a real sensor by adding some measurement errors. It has been used the same model of the Sun sensor:

- Misalignment error: $A_\epsilon = I - [\theta_\epsilon]^\wedge$, where we have assumed $\theta_\epsilon = 0.166^\circ$ due to the sensor accuracy.
- Zero-Order Hold, which mimics the sampling acquisition frequency of the sensor: *Sample time* = 0.1
- Band-Limited White Noise, which represents errors in the values read by the sensors' electronics: *Noise power* = 0.00001 and *Sample time* = 0.1

3.3 Gyroscopes

The onboard presence of gyroscopes is essential for the de-tumbling phase: the objective of this phase is to reduce the angular velocity of the spacecraft almost to zero; in order to do that, it is mandatory to know the instantaneous angular velocity of the s/c. Since the spacecraft is rotating randomly around its axis with an angular velocity higher than the stationary one, the Sun sensors and the Horizon sensors cannot work properly, hence they cannot determine the attitude of the spacecraft, from which it could be possible to deduce the angular velocity. Therefore it was decided to equip the spacecraft with the STIM300 from Safran Sensing Technologies; this sensor comprehend a set of 3 highly accurate gyros, which allow us to obtain directly the angular velocity in the body reference frame (ω_B).

The errors due to the action of non-ideal gyroscopes has been modeled according to the following equation:

$$\omega_{B/N}^m = A_\epsilon \omega_{B/N} + ARW + RRW \quad (3.4)$$

Where ARW and RRW, respectively the Angular Random Walk and the Bias Instability, are information provided from the manufacturers. For the STIM300: $ARW = 0.15^\circ/\sqrt{h}$ and $RRW = 0.3^\circ/h$.

The misalignment matrix was instead defined as: $A_\epsilon = I - [\theta_\epsilon]^\wedge$, where we have assumed $\theta_\epsilon = 0.04^\circ$ due to the accuracy.

3.4 Actuators

A set of four variable thrust jets has been provided to the spacecraft in order to guarantee the attitude control.

The general configuration of Figure 3.1 shows the map of the forces generated by 4 thrusters.

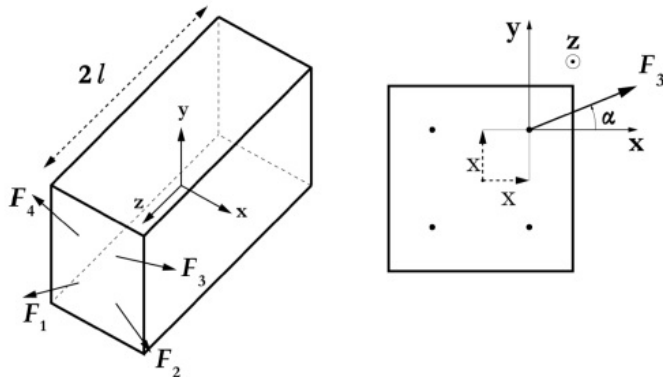


Figure 3.1: Generic configuration of actuators

We have however decided to place the actuators in the corners of the face with an inclination α of 45° in order to maximise the lever arms. The total torque generated can be expressed as:

$$\underline{T}_{tot} = [\hat{\underline{R}}]\underline{F} \quad (3.5)$$

Where $\hat{\underline{R}}$ is a matrix that maps the the force generated by the set of thrusters into the torque with respect to the body axes and \underline{F} is the matrix of forces that the actuators need to achieve

in order to grant the total torque required by the control system.

In our specific case the \hat{R} matrix result to be:

$$\hat{R} = \begin{bmatrix} \frac{w}{2}\sin(\alpha) & 0 & 0 \\ 0 & \frac{w}{2}\cos(\alpha) & 0 \\ 0 & 0 & \frac{d}{2}\sin(\alpha) - \frac{d}{2}\cos(\alpha) \end{bmatrix} \begin{bmatrix} 1 & 1 & -1 & -1 \\ -1 & 1 & 1 & -1 \\ 1 & -1 & 1 & -1 \end{bmatrix} \quad (3.6)$$

Since \hat{R} is not a square matrix it's not possible to invert the equation in order to directly obtain \underline{F} , knowing the ideal desired total torque (M_{ideal}). It is necessary to apply the Moore-Penrose pseudo inverse so that is possible to define \underline{F} as:

$$[\underline{F}] = [\hat{R}]^* M_{ideal} + \gamma w \quad (3.7)$$

$$\gamma = \max_{i=1,\dots,N} \frac{([\hat{R}]^* M_{ideal})_i}{w_i} \quad (3.8)$$

where $w > 0$ is the null space vector of \hat{R} .

As previously done for the sensors, we have modeled the real actuators by adding some measurement errors:

- Band-Limited White Noise, which represents errors in the values read by the sensors' electronics: *Noise power* = 0.00001 and *Sample time* = 10.
- Rate limiter, which limit rising and falling rates of signal: *Slew rate* = ± 500 .
- Saturation, which limit input signal to the upper and lower saturation values: *Upper limit* = 0.15 and *Lower limit* = 0.

Chapter 4

Attitude determination

4.1 Introduction

As we said previously, the sun sensor is not sufficient to completely determine the attitude of our spacecraft. It requires at least one further scalar measurement, taken from the horizon sensor. In our case the solution can be obtained with the following algebraic method.

Call the two measurements p and q , and call a and b their corresponding directions in inertial space. Associate the measurement p to unit vector s_1 and the corresponding direction a to unit v_1 . Two orthogonal frames can then be associated to the measurements and to the reference directions as follows:

$$s_1 = p \quad s_2 = \frac{p \times q}{|p \times q|} \quad s_3 = p \times s_2 \quad (4.1)$$

$$v_1 = a \quad v_2 = \frac{a \times b}{|a \times b|} \quad v_3 = a \times v_2 \quad (4.2)$$

Since by construction the 3 unit vectors s_1 , s_2 , s_3 and v_1 , v_2 , v_3 are orthogonal, we can write:

$$V^{-1} = V^T \quad (4.3)$$

$$A = SV^{-1} = SV^T \quad (4.4)$$

To minimize the errors, vector p should be measured with the maximum possible precision and q should be as orthogonal to p as possible. For this reason, we have chosen a very precise sun sensor, the S3 (Smart Sun Sensor) from Leonardo company and the Horizon sensor from SolarMems technologies, whose measurement is orthogonal to that of the sun sensor. In fact in order to work, this method requires that the two vectors must be linearly independent and this is guaranteed by the polarity of the orbit.

Figure 4.1 shows that the estimated DCM is very accurate, thanks to both the high precision of the sensors and the method used to compute them.

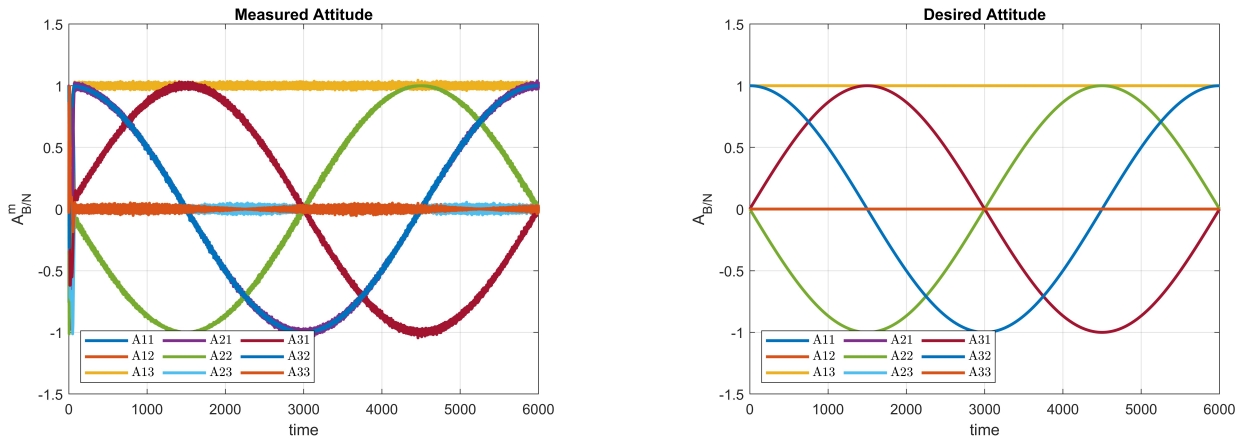


Figure 4.1: Comparison between Measured Attitude and Desired Attitude

4.2 Control Algorithms

In order to control the spacecraft from separation from the launcher to its nominal nadir-pointing phase, we use three different control strategies. For the de-tumbling phase, we use a nonlinear de-tumbling controller and, when the angular velocity has been lowered enough, a non linear control algorithm based on Lyapunov's second stability theorem is used for the slew manoeuvre. In the nominal phase we use a simple linear controller (PD).

4.2.1 De-tumbling

After the separation from the launcher, the first operation the spacecraft needs to perform is the de-tumbling. This manoeuvre aims to reduce the satellite's residual angular velocity, without any constraints on the orientation at the end of the procedure. In our case the sensors can't guarantee knowledge of the attitude and angular rates even for relatively low angular velocities and for this reason we are using the gyro sensor (STIM 300) from Safran Sensing Technologies. The control proportional to the estimated ω allows us to reach the desired total angular rate (very low) unless for even small angular velocities the sun sensor cannot work. The proportional controller where the control input u , identified as the desired (ideal) torque, is proportional to the measured ω of the gyroscopes as said before.

$$\underline{u} = -k\underline{\omega} \quad (4.5)$$

The gain was chosen with a tuning method, i.e. iterations until we found an adequate value that would bring the angular velocities to zero in a certain time. We carried out tests by changing the value of the coefficient k until convergence to zero was guaranteed.

As we can see in the figure below, the control action guarantee the stability of the angular velocities in less than a minute when using a $k = 0.5$.

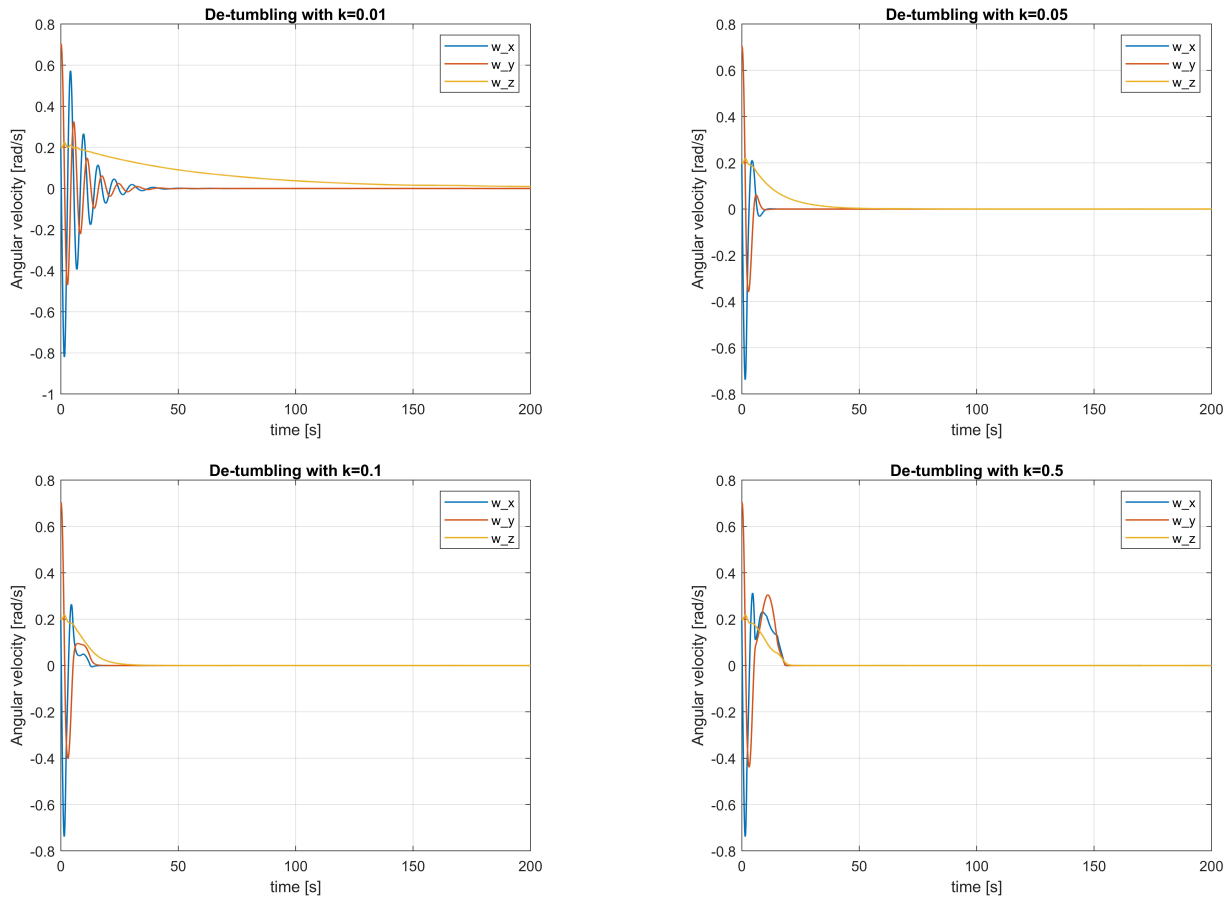


Figure 4.2: De-tumbling effect on the angular velocity

4.2.2 Slew manoeuvre

When the spacecraft reaches a sufficiently low angular velocity, the next manoeuvre can be performed in order to recharge the battery. In our Simulink model we decided to switch from the de-tumbling to the slew manoeuvre after a certain time (40 seconds) in which we are certainly sure that the de-tumbling is finished. The objective of this mission is to perform Earth observation, hence a slew manoeuvre and a subsequent nadir-pointing control needs to be designed. The algorithm of choice is based on Lyapunov's function for a DCM control:

$$V = \frac{1}{2} \underline{\omega}^T I \underline{\omega} + k_2 \text{tr}(I_3 - A) \quad (4.6)$$

A slew motion is defined as a controlled motion between two attitudes. The starting attitude is random, while in our case the final attitude is the nominal desired attitude because we are on a sun-synchronous orbit. In this we can both recharge the batteries and carry out earth observation.

The required control action, according to Lyapunov's second stability theorem is defined by the following equation, where $\underline{\omega}_d$ is the vector of the desired angular velocities. The reference frame is the LVLH and it changes slowly, so the term $I(A_e \dot{\underline{\omega}}_d - [\underline{\omega}_e]^\wedge A_e \underline{\omega}_d)$ can be neglected.

$$\underline{u} = -k_1 \underline{\omega}_e - k_2 (A_e^T - A_e)^V + \underline{\omega} \times I \underline{\omega} + I(A_e \dot{\underline{\omega}}_d - [\underline{\omega}_e]^\wedge A_e \underline{\omega}_d) \quad (4.7)$$

The exponent V is the “inverse hat” operator: $(X_{3 \times 3})^V = [X_{32} X_{13} X_{21}]^T$.

In order to choose the adequate gains k_1 and k_2 , also in this case we used a tuning method. We started using casual values of the gains:

$$k_1 = 1 \quad k_2 = 1 \quad (4.8)$$

The final values are:

$$k_1 = 1 \quad k_2 = 0.05 \quad (4.9)$$

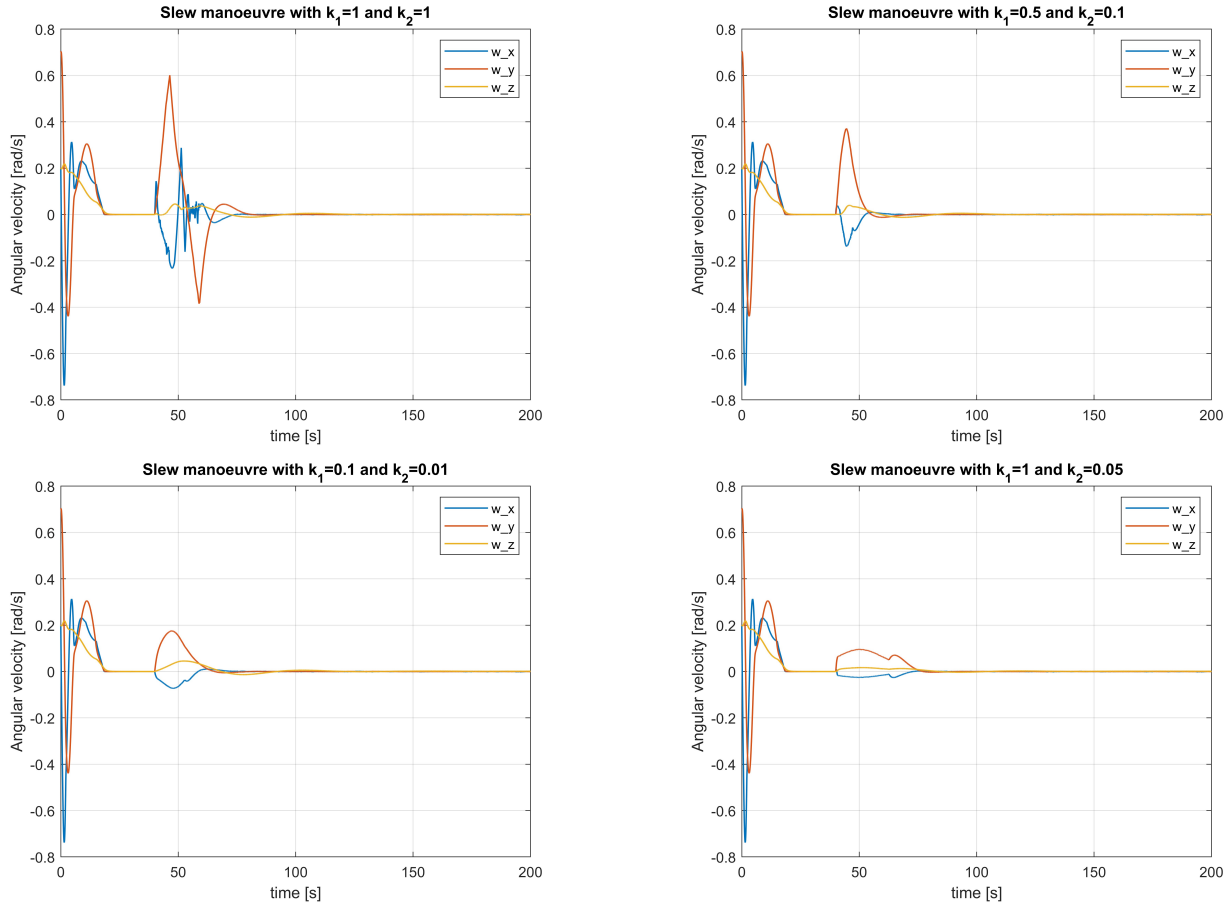


Figure 4.3: Slew manoeuvre effect on the angular velocity

4.3 Nominal control logic

4.3.1 References for tracking

For a tracking manoeuvre two references are necessary, one for the attitude and one for the angular velocity:

$$\underline{\omega_d} = \begin{Bmatrix} 0 \\ 0 \\ \sqrt{\frac{\mu}{a^3}} \end{Bmatrix} \quad A_{target} = \begin{bmatrix} 1 & 0 & 0 \\ 0 & 1 & 0 \\ 0 & 0 & 1 \end{bmatrix} \begin{bmatrix} 0 & \cos(\theta) & \sin(\theta) \\ 0 & -\sin(\theta) & \cos(\theta) \\ 1 & 0 & 0 \end{bmatrix} \quad (4.10)$$

Where the first matrix of A_{target} correspond to $A_{B/L}$ and the second one correspond to $A_{L/N}$.

The error matrix used by the controller is then computed as the product between the estimated and the desired attitude matrices.

$$A_e = A_{B/N}^m A_{target}^T \quad (4.11)$$

Our goal is to obtain $A_e = I$.

4.3.2 Control implementation

In our Simulink model, the nominal control logic starts when we reach an angle small enough and it switches from the slew manoeuvre to the final control logic. The threshold is set to $\alpha_{err} = 0.3$, where α_{err} is a scalar parameter that represents the angular error with respect to the desired attitude, and has been defined as follows:

$$\alpha_{err} = \text{trace}(I - A_e) = \text{trace}(I - A_{B/N}^m A_{target}^T) \quad (4.12)$$

The controller for the nominal condition is a PD controller. We want to relate the attitude error with the control torque, in order to satisfy our goal $A_e = I$.

Since $A_e = \begin{bmatrix} a_{11e} & a_{12e} & a_{13e} \\ a_{21e} & a_{22e} & a_{23e} \\ a_{31e} & a_{32e} & a_{33e} \end{bmatrix}$, our control torque in a general case will be:

$$\begin{cases} M_{xS} &= \frac{K_{px}}{2}(a_{23e} - a_{32e}) + K_{dx}\omega_x \\ M_{yS} &= \frac{K_{py}}{2}(a_{31e} - a_{13e}) + K_{dy}\omega_y \\ M_{zS} &= \frac{K_{pz}}{2}(a_{12e} - a_{21e}) + K_{dz}\omega_z \end{cases} \quad (4.13)$$

Also in this case the gains were chosen by carrying out tests (tuning) until we found a value that stabilized our model in an optimal way. We used the same gain for each axis.

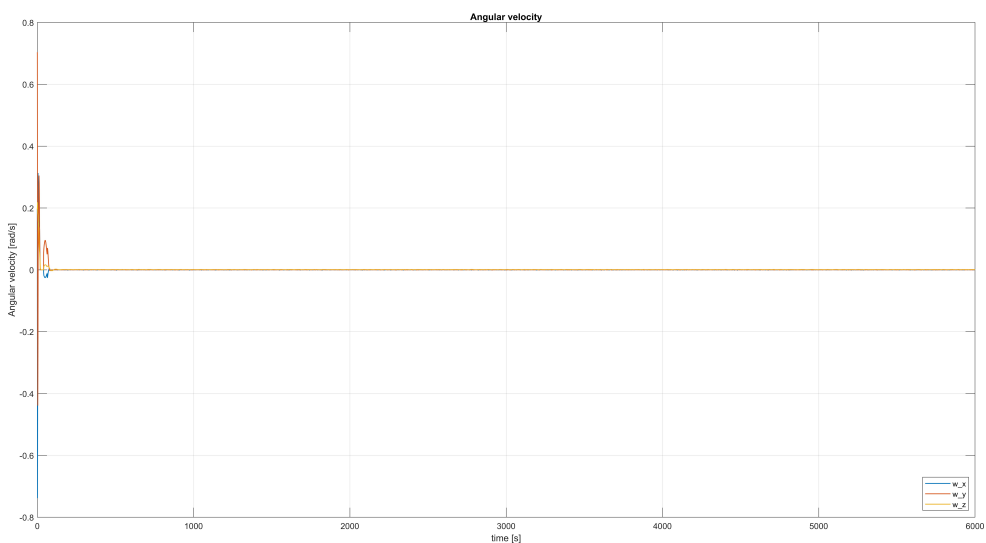
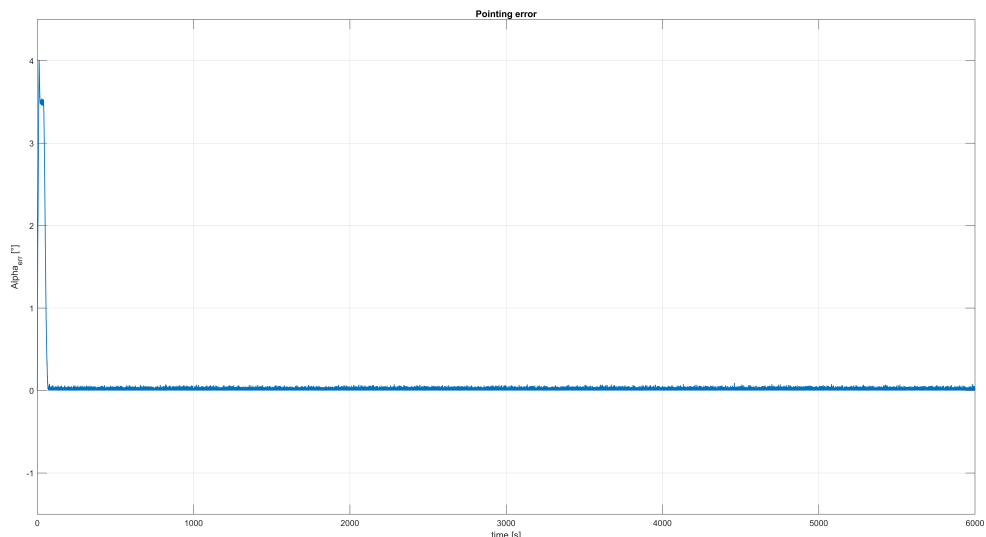
The final values are:

$$K_{px} = K_{py} = K_{pz} = 0.01 \quad K_{dx} = K_{dy} = K_{dz} = 0.05 \quad (4.14)$$

Chapter 5

Conclusion

The final results for the pointing error and the angular velocity are shown below, together with the error matrix A_ϵ :



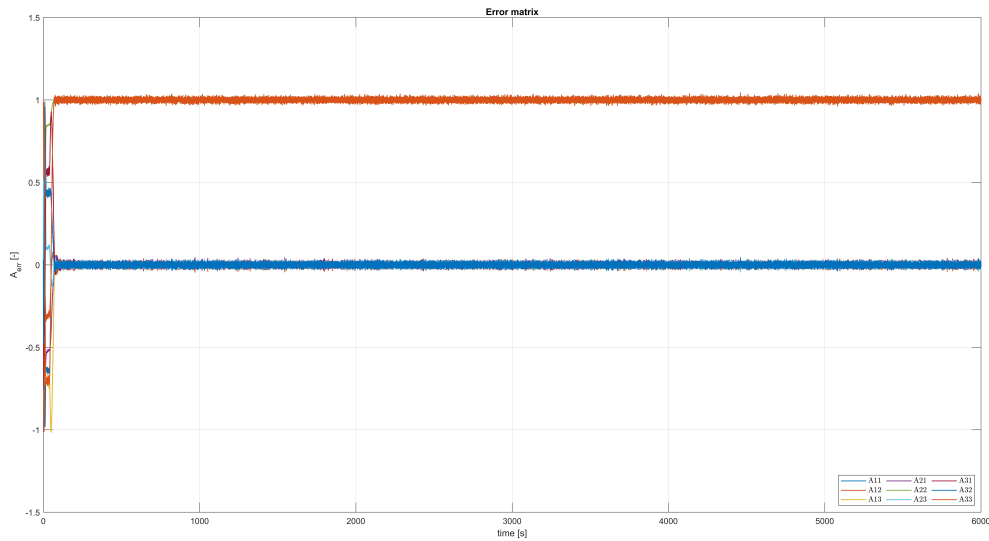


Figure 5.1: Final results

The control logics, as we can see from the graphs, fully satisfy the objectives of our mission, with an error matrix that becomes an identity matrix and the angular speeds that have very small oscillations.

Bibliography

- [1] F. Bernelli, *Notes for spacecraft attitude dynamics and control course.*
- [2] S. Schalkowsky, M. Harris, *NASA SP-8018 : Spacecraft magnetic torques.*
- [3] Abby Tabor, *What is BioSentinel?.*